Version of Record: https://www.sciencedirect.com/science/article/pii/S0959440X23001367
Manuscript_a493c74dabf1b67ae8f436775c80c6e8

Radiation damage to biological macromolecules

[1]Elspeth F Garman and [2]Martin Weik

1Department of Biochemistry, Dorothy Crowfoot Hodgkin Building, South Parks Road, Oxford, OX1 3QU, UK
[2]Univ. Grenoble Alpes, CEA, CNRS, Institut de Biologie Structurale, F-38044 Grenoble, France

Keywords: radiation damage, X-rays, dose, global damage, specific structural damage, reduction, disulphide bond breakage, synchrotrons, electrons, microscopy

Abstract
In this review we describe recent research developments into radiation damage effects in macromolecular X-ray crystallography observed at synchrotrons and X-ray free electron lasers. Radiation damage in small molecule X-ray crystallography, small angle X-ray scattering experiments, microelectron diffraction, and single particle cryo- electron microscopy is briefly covered.

Introduction
Radiation damage (RD) is now a main-stream concern in macromolecular crystallography (MX), with an increasing awareness of its effects on biological interpretations of X-ray and electron microscopy derived structures, and a wider appreciation of its effect on data collection strategies. The origin of these effects is that the samples absorb the incident radiation due to the photoelectric and Compton effects, as well as scattering them elastically: the latter is the 'useful' signal obtained during data collection, but the former results in loss of energy by the incident radiation and thus damage to the irradiated material. The initial absorption is known as a 'primary event' and the subsequent cascade of product formation as 'secondary events'. Electrons and X-rays interact differently with atoms so the precise damage mechanisms differ. However, in all cases the primary event is an unavoidable fact of physics, whereas the extent of the secondary events (*i.e.,* chemical and structural changes) is both time and temperature dependent, so that these are partially mitigated by cryocooling the sample (usually to around 100 K[1]). In MX experiments, the crystals typically contain a large percentage by volume of the water and precipitant in which the protein crystals are grown. These components suffer radiolysis which can subsequently cause 'indirect' damage, whereas absorption of an X-ray by the macromolecule leads to 'direct damage' (see Figure 1). The damage effects are observable in both reciprocal and real space and are labelled 'global' and 'specific' RD, respectively, and their progression is usually monitored as a function of the absorbed dose (energy absorbed/mass=J/kg=Gy, gray).
The driving interest in understanding RD effects in the different methods used to determine macromolecular structures is that unfortunately they can change the observed data, and thus mislead or confound, biological interpretations. Some examples of radiation induced changes are domain swapping in human cystatin C[2], transformation of growth factor beta-1 activation•[3], generation of polymorphism (crystals with different unit cells for the same protein) and photoreduction in metalloproteins[4, 5], especially in haem containing proteins[6], active-site geometry changes in a lytic polysaccharide monooxygenase[7], reduction of compound 1 of the iron containing Catalase-3[8] and photoreversible interconversion of a phytochrome photosensory module[9]. There is some evidence that active sites of enzymes are particularly radiation sensitive, perhaps due to strain caused by readiness for action[10]. While such X-ray induced effects are mostly a nuisance,

they can also be put to good use for studying macromolecular reaction mechanisms, particularly those involving redox changes that can be triggered by X-ray generated electrons. Besides seminal work on cytochrome p450cam[11] and horseradish peroxidase[12], recent examples include the study of oxygen reduction and water release from the active site of a laccase[13]. When monitoring X-ray induced effects, *in crystallo* optical-spectroscopy techniques (absorption, fluorescence, Raman) have proven a very informative complement to MX[14, 15], especially when studying very radiation sensitive proteins containing metal centres or conjugated π-systems.

X-ray radiation damage at cryotemperatures

During MX experiments carried out at cryotemperatures (usually around 100 K), RD manifests itself in reciprocal space as progressive diffraction intensity loss, high resolution reflections disappearing first, unit cell volume and scaling B-factor increase, worsening internal data merging statistics, and often increased crystal mosaicity. In real space, for the resulting structures, atomic *B*-factors (temperature factors) rise with dose, and more importantly, some amino acids and ligands such as metal atoms are preferentially damaged before others. This specific RD has been well characterised in a large range of proteins and follows a defined and reproducible order: metal-centre reduction, disulphide-bond cleavage (~0.2 MGy), acidic residue decarboxylation (~4 MGy) and electron loss around the sulphur atom of methionine residues (Ian Carmichael, unpublished communication), as well as some side chain disordering. Although scission of tyrosine -OH was also previously suggested, observed electron density differences seen round this moiety have now been attributed to movement of the whole side chain[16]. At cryo-temperatures, global RD becomes evident in the diffraction data only at much higher doses than the appearance of specific RD[17]•[18]. These reciprocal and real space RD effects at 100 K are summarised in Figure 2.

While RD in protein crystals has been well studied over the past 20 years, much less attention has been paid to the effects in DNA and RNA crystals. A recent study concluded that compared to the rate of damage to lysozyme crystals from which data were collected under identical conditions, the 16-mer DNA crystal was less sensitive to both global and specific RD•[19].

There are a number of possible causes of the RD pathologies observed at 100 K, including crystal heating. Recent studies using 20-40 μm ruby crystals concluded that the temperature rise induced by current synchrotron beam sizes and flux densities was around 20 K[20]. Above 110 K it is possible that OH radicals are mobile[21] and could thus induce new damage features and accelerate the rate of RD[22], so with the ever increasing fluxes of 4th generation synchrotrons, this effect may become a critical factor to consider for crystal lifetimes. So far the dose rate has not been found to affect the rate of progression of RD at 100 K (up to ~50 MGy/s[23]) but this conclusion will require revisiting for the flux densities now available.

Continued effort to derive a model to characterise the reciprocal space RD induced diffraction intensity decay at both RT and cryo-temperatures has made some recent progress on developing an approach with physical significance•[24].

Interestingly, specific RD susceptibility within each residue type follows a preferential ordering influenced by a combination of local environment factors (solvent accessibility, conformational strain, proximity to active sites/high X-ray cross-section atoms[25]). Deconvoluting the individual roles of these parameters has been surprisingly challenging, but the reason for this differential damage for disulphide bonds has lately been investigated in several proteins•[26]. The susceptibility to bond

reduction was found to be correlated with its proximity to a carbonyl oxygen atom positioned along the extension of the S-S bond vector, predisposing electron transfer from the oxygen atom to the disulphide bond. Regarding oxidative damage, cysteine modification has recently been described[27] in addition to the well documented decarboxylation of acidic residues. Specifically, a reactive cysteine near a water molecule has been proposed to yield a Cys-SOH moiety in a hydroxyl radical-mediated photo-oxidation reaction[27].

X-ray radiation damage at room temperature

RD at room temperature (RT) was first investigated in 1962[28] and reflection intensity loss was modelled. In reciprocal space, global RD effects at RT are qualitatively similar to those for 100 K data collection mentioned above, yet their progression is observed to be two orders of magnitude faster[22, 29]. From the early observation that some reflection intensities increased with dose, it was conjectured that specific RD occurs[28]. Decades later, this was indeed observed in RT electron density maps, specifically the breaking and disordering of disulphide bonds[30]. Since then, serial synchrotron crystallography (SSX) approaches (e.g.[4, 31, 32]•[33]) have been developed that allow distribution of absorbed dose over thousands of microcrystals, thereby increasing the dose efficiency of data collection and enabling more widespread use of RT X-ray crystallography (reviewed by[34], and see April 2023 special issue Acta Cryst. D79). Whereas the RT breakage of disulphide bonds has been confirmed[35-38]•[33], evidence for radiation induced decarboxylation of acidic residues has not yet been presented. Interestingly, it was recently reported that specific and global radiation damage evolve on a similar dose scale at RT, unlike at cryo-temperatures, where they are much more decoupled•[18]. The coupling of both types of RD at RT makes observation of specific RD in electron density maps much more challenging than at cryo temperatures, as at RT global RD destroys crystalline order at lower absorbed doses[37]. Consequently, some studies report specific RD observed in Fourier difference electron density maps[35-38]•[33], while others do not[39]•[18]. Lately an X-ray topographic study at RT showed that specific crystal defects, such as dislocations, occur at similar doses as does global RD[40].

At RT, the dose at which the diffraction intensity is halved with respect to the zero-dose intensity ($D_{1/2}$) has been estimated to be 0.1–1.2 MGy for a variety of protein crystals, grown in various conditions and diffracting to a range of resolutions (see references in[33] for comprehensive $D_{1/2}$ review), *i.e.* two orders of magnitude lower than the $D_{1/2}$ at 100 K of around 10 MGy reported for lysozyme crystals diffracting to 1.6 Å resolution[41] and the $D_{0.7}$ limit of 30 MGy at 2.2 Å for holo and apo-ferritin crystals[17]. At 100 K, specific RD was observed to be so significant at $D_{1/2}$ that adopting a lower limit of $D_{0.7}$ was recommended[17]. Unlike at 100 K, a dose rate effect has been reported at RT whereby the $D_{1/2}$ increases by around a factor of 2 at ~49 MGy/s compared to at ~50 kGy/s[23], while a recent SSX study at 2.4 and 40.3 MGy/s only observed a marginal dose rate effect•[33]. The dose rate effect issue at RT is thus still a matter of debate.

Macromolecular structures determined from X-ray crystallographic RT data collected display different, functionally more relevant conformational heterogeneities than those determined from cryo-data[42]. Importantly, conformational heterogeneity does not appear to be influenced by RD at RT[37, 43], while it does at cryo-

temperatures[43]. Specifically, RD-induced appearance, disappearance and redistributions of side-chain rotameric states are observed at 100 K, but not at RT, possibly because global RD limits the RT diffraction quality before these can be detected[43]. While it is more challenging to collect crystallographic data at RT rather than at cryo-temperatures because of increased radiation sensitivity, the conformational heterogeneity of the resulting structural models is not only functionally more relevant, but is also less biased by radiation damage at RT than at 100 K.

Detecting radiation damage in PDB deposited structures

The Protein Data Bank (PDB) contains over 200,000 experimentally determined macromolecular structures and during 2022 there were on average 811,037 structures downloaded/day, 563/min(https://www.wwpdb.org/stats/download). Currently the PDB file metadata contains no information allowing assessment of the level of structural RD effects. Only by calculating difference electron density maps between the diffraction data (now mandatorily deposited) and the model can specific RD to the amino acids be observed. We estimate that only roughly 10% of researchers using PDB structures have crystallographic training and thus have understanding of the PDB quality indicators. Thus, RD artefacts are likely to remain largely unnoticed.

However, a new RD metric, B_{net}, has been developed enabling a PDB deposited cryo-cooled structure to be given a single number indicating its extent of damage. B_{net} is derived from the distribution of the structure's per atom B_{damage} values, calculated by deconvoluting the local packing density from the atomic *B*-factors [44]. Recently B_{net} values were calculated for 93,978 PDB structures and they ranged from <1 to 96. Those with B_{net}>3 (~5% of total) consistently showed specific RD, as did ligand bound structures with B_{net}>1.5••[45].

Experimental strategies for minimising X-ray radiation damage

In addition to understanding and predicting RD progression, a major aim of MX RD research is to find mitigation strategies so that experimenters can collect reliable diffraction data with minimum RD. Various ideas have been proposed and tested to extend the dose lifetime of protein crystals. For robust results that can be properly compared to assess the effectiveness of a particular approach, dose must be estimated as accurately as possible (see below). Pipelines for optimising data collection strategies can include calculation of dose (e.g. by DOZOR at MASSIF-1, ESRF[46] and KUMA in ZOO, the SPring-8 automatic data collection system[47]). RADDOSE-3D is a software tool that now allows time and space resolved absorbed doses to be computed for a range of experimental methods[48, 49] and it is now implemented at a number of synchrotron beamlines (e.g. I04 at DLS, BL12-1 and BL12-2 at SSRL) allowing a total dose rather than a total time to be specified for a data collection.

From the experimentalist's point of view[50], having awareness of the factors affecting absorbed dose and thus RD progression is important in order to mitigate it. For instance, the increased absorbed dose caused by non-ordered heavier atom crystallisation buffer components (e.g., arsenic in cacodylate buffer) can be back-soaked out before cryo-cooling the crystal, extending the crystal lifetime. Ensuring even dose spreading over 'fresh' crystalline macromolecules is a very effective approach for minimising both specific and global RD. This can be achieved either by a helical irradiation scheme [51] or by multi-crystal[52] or serial crystallography••[4].

Note that MX using non-ionising neutrons yields damage free structures[53, 54]. Importantly, the development of serial femtosecond crystallography([55]SFX) at X-ray free electron lasers (XFEL) circumvents many issues arising from RD effects (see below).

Using higher incident X-ray energies, E_x, could reduce RD effects, especially for microcrystals from which photoelectrons could escape and thus not contribute to absorbed dose[56]. As E_x increases, both elastic scattering and photoelectric cross sections decrease, whereas the Compton cross section increases. Monte Carlo simulations including the higher detective quantum efficiency (DQE) at higher E_x of new CdTe pixel detectors predicted an optimum diffraction efficiency (DE: total number of elastically scattered photons/absorbed dose in MGy) at 26 keV[57]. Experimental validation of this idea has recently been achieved in two studies[58]••[59]. As predicted by simulations[57], the DE increased by a factor of more than two at 25 keV compared to 12.4 keV, and the resolution to which data could be collected for the same dose was better••[59].

Importantly, specific RD as a function of E_x has also been investigated for $10< E_x <30$ keV using multiple crystals of highly radiation sensitive cryocooled cytochrome c oxidase and very low doses (55 kGy), and a CdTe detector with on-line UV-vis absorption spectra measurements. No E_x dependence of specific damage was found, and the ligand structure bond-length reproduced an RD-free XFEL structure[60].

Challenges in estimating the dose

As mentioned above, the usual *x*-axis metric against which RD effects are plotted is the absorbed dose. However, the dose cannot be measured, it can only be estimated from knowledge of the crystal size and content (#amino acids, #of non-organic heavier atoms, solvent components), and the beam parameters (size, flux, profile, energy), most of which carry experimental errors. Thus, there is often significant uncertainty in resulting dose values. Another critical issue is which dose should be quoted, since it can vary over a very large range within one sample due to the profiles of synchrotron beams, which are typically Gaussian-like rather than 'top-hat' in shape (see Figure 3). Options for dose specification include: maximum dose, average dose for the whole crystal volume, average dose where 95% of the energy is deposited, and diffraction weighted dose, DWD[61]. DWD combines information from the aggregation of dose within each crystal volume element up to that time, with the way the crystal is being exposed at that moment. A modification of DWD to include an intensity decay model was suggested[62], and it has now been shown that appropriate models are highly dependent on the beam shape. For Gaussian-profile (rather than top-hat shaped) beams, such a modified DWD becomes almost independent of actual dose at large doses because damaged regions no longer diffract to high resolution[23]. Note that most nominally 'Gaussian' shaped synchrotron beams are not truly Gaussian. For instance, a recent detailed RT analysis of damage progression to a disulphide bond clearly demonstrated the non-linear effects produced by inhomogeneous X-ray irradiation in a pseudo-Voigt (Gaussian with Lorentzian tails) distribution•[33]. Because of 'hole burning' by the intense beam centre[23], disulphide bonds were first damaged and then appeared to recover with dose•[33].

Radiation damage in serial crystallography at bright X-ray sources

In a typical serial crystallography experiment, the absorbed dose is spread over thousands of macromolecular microcrystals, thereby efficiently minimising the total dose of a full data set composed of patterns each collected from an individual crystal. In serial synchrotron crystallography (SSX) experiments, the total absorbed dose per dataset can be as low as a few kGy•[33], although specific radiation damage cannot be completely avoided, as monitored e.g. *via* the length of radiation sensitive iron – ligand bonds in crystalline P450nor at 100 K[63] and a heme peroxidase at RT••[4]. Only the use of femtosecond X-ray pulses produced in XFELs allows radiation damage to be outrun in SFX experiments[55]. These have yielded the 'true' iron – ligand bond length as verified by zero-dose extrapolation of dose-dependent SSX data••[4] and quantum chemical calculations[63]. Recent examples of damage-free structures determined by SFX include those of flavin containing enzymes[64, 65] and another metallo-protein[66]. Whereas RD is generally outrun in SFX experiments (reviewed in[67]), both global[68] and specific[69] RD can be observed if long (e.g. 80 fs: compare with the typical lengths of 35 fs (LCLS) and 10 fs (SACLA)), unattenuated XFEL pulses are employed. Specific RD to disulphide bonds has been generated and visualised in time-resolved X-ray pump/ X-ray probe SFX experiments on protein nanocrystals, providing real time insight into X-ray induced bond elongation••[70]. Femtosecond time-resolved absorbed doses can be estimated with RADDOSE-XFEL•[71].

Radiation damage in small-angle X-ray scattering

RD is also a major consideration when designing small angle X-ray scattering (SAXS) experiments, most commonly performed on solutions held at RT. On X-ray irradiation, the sample can aggregate or denature, giving misleading results. Mitigation strategies include flowing the liquid across the beam, careful analysis of pairwise agreement between consecutive frames of data to monitor degradation, and frequent change of static samples[72]. A recent SAXS study on a protein engineered to dimerise through a susceptible disulphide bond observed a dimer-to-monomer dose-dependent X-ray induced bond cleavage and fragmentation: a low dose transition under near physiological conditions, which was also affected by the solution pH. Thus the radiation chemistry known to occur in MX was applied predictively to useful effect•[3].

Radiation damage in small molecule X-ray crystallography

Since the advent of synchrotron beamlines designed for small-molecule crystallography (SMX), SMX researchers have become aware of RD artefacts in their structures. The absorption coefficients of some SMX samples at E_x=8 and 18 keV (where data are commonly collected) can be up to 2x and 10x that for MX crystals, respectively, due to their often higher metal content, resulting in higher doses for the same beam conditions compared with MX. Radiation chemistry effects are somewhat different, since SMX samples are hydrates or contain 1–10 molecules from the crystallisation solvents, whereas MX samples can comprise up to 80% water.

Three recent SMX RD studies reported similar global RD effects to those in MX. SMX atomic models suffer from increased thermal ellipsoids, elongation of some bond lengths resulting in less reliable molecular geometry, and gradual disordering of the bound water[73-75]. A major conclusion was that SMXers should try to select an E_x below the relevant metal atomic absorption edge. As for MX, SMX RD can be mitigated with XFEL serial crystallography[76].

Radiation damage in microcrystal electron diffraction and single-particle cryo-electron microscopy

As with X-rays, electron beams represent ionising radiation that can generate RD in biological macromolecules [77], thus posing challenges for microcrystal electron diffraction (MicroED) and single-particle cryo-electron microscopy (EM) experiments. Whereas global electron RD in single particle cryo-EM was observed and well described[77] prior to the 'resolution revolution'[78], specific RD effects, particularly at negatively charged residues, were only noted more recently[79]. In fact, RD imposes a fundamental lower limit on the molecular mass of proteins that can be successfully investigated [80]. Lately, specific RD has been analysed in high-resolution cryo-EM structures of PSII and compared with damage free SFX structures•[81]. The radiation-induced elongations of Mn-Mn and Mn-O bonds observed in the cryo-EM structures could be reduced, but not eliminated, by limiting the total exposure to 3.3e^-/Å^2 (corresponding to 12.2 MGy according to[77]). Further mitigation of radiation damage might be achieved through using 100 keV rather than 300 keV electrons[82], cooling the sample to liquid-helium rather than liquid-nitrogen temperature[83], or by using alternative schemes to improve dose efficiency[84]. In conjunction with movement free small hole gold grids, extrapolation of structure factor decay in reciprocal space back to zero-dose has been shown to be effective[85].

In MicroED, macromolecular nanocrystals are presented under cryo-conditions to the electron beam and crystallographic rotation data collected[86]. A systematic MicroED study has presented evidence for both global and specific electron beam damage••[87]. The average intensity of all reflections in proteinase K nanocrystals decreased to 73% of its extrapolated zero-dose value after exposure to 1 e^-/Å^2. According to[77], this fluence corresponds to 4.5 MGy, which is lower than the $D_{0.7}$ yardstick of 30 MGy in X-ray cryo-crystallography[17], possibly because the two studies were at different resolutions. Site-specific electron RD to metal sites, disulphide bonds and acidic amino acid side chains has been observed at exposure values below 1 e^-/Å^2, with a similar ranking of radiation sensitivity as observed in X-ray cryo-MX[87]. The specific RD to a Zn atom has been used for experimental phasing of MicroED data[88], similarly to an approach applied in X-ray crystallography [89]. Of note is that the absorbed dose can be fractionated by a serial approach to electron diffraction, thereby minimising RD[90] similarly to SSX and SFX.

In MicroED and single-particle cryo-EM, the reported dose is most often expressed in e^-/Å^2. Efforts to express these doses in gray (as e.g. in[81] and[84]) would facilitate a more systematic RD comparison in both X-ray and cryo-EM. The dose (in gray) absorbed by protein samples as a function of electron exposure and accelerating voltage can be estimated using table 15.1 in[77] or by using the simplified formula proposed in[91] based on the near constancy of stopping power per atomic electron, which gives estimates accurate to within around 5%. For comparing RD effects in MicroED and single-particle cryo-EM the availability of a simple tool to allow doses to be specified in gray would be beneficial.

Conclusion

The topic of radiation damage to biological macromolecules in X-ray and electron scattering, diffraction and imaging experiments has steadily increased in its relevance and recognition as an important challenge over the past few decades and

it now constitutes a mainstream field of research. There remains a need to continue systematic investigation of RD effects to improve our understanding of the issues, especially with more 4th generation synchrotrons with ever brighter beams coming online (Figure 4). For instance, it is likely that the increased X-ray beam induced heating at these sources will become an issue in cryo-MX experiments, by inducing a dose-rate effect through liberating radicals that are trapped at 100 K. Related to this, there is a pressing need to deconvolute radiation induced changes from non-equilibrium dynamics in time-resolved SSX experiments. After some successful initial studies[69]••[70], global RD and specific radiation induced changes in crystalline and non-crystalline biological macromolecules at XFELs will need further assessment. To realise the full potential of single particle cryo-EM, maximising the dose efficiency is the most effective strategy, and continued developments to achieve this will undoubtedly expand the capabilities of the technique in the future. More generally, it is anticipated that opportunities will multiply for the complementary use of X-ray crystallography (MX, SSX, SFX), neutron crystallography and cryo-EM (MicroED and single-particle) to assess and minimise radiation damage in integrated structural biology projects[54, 81]. The future of X-ray and electron scattering experiments in structural biology is bright, but we must maintain and further extend the spotlight on the various radiation damage issues discussed in this review.

Acknowledgments
We thank Ian Carmichael and Joshua Dickerson for critical and constructive reading of the manuscript. Sean McSweeney and Robert Fischetti are acknowledged for the idea (in 2016) behind Figure 4. We thank the many synchrotron scientists internationally for providing up-to-date beamline parameters. We thank colleagues for help with figures: Kathryn Shelley (Figure 2), Charles Bury (Figure 3) and Nicolas Coquelle (Figure 4).

Figures :

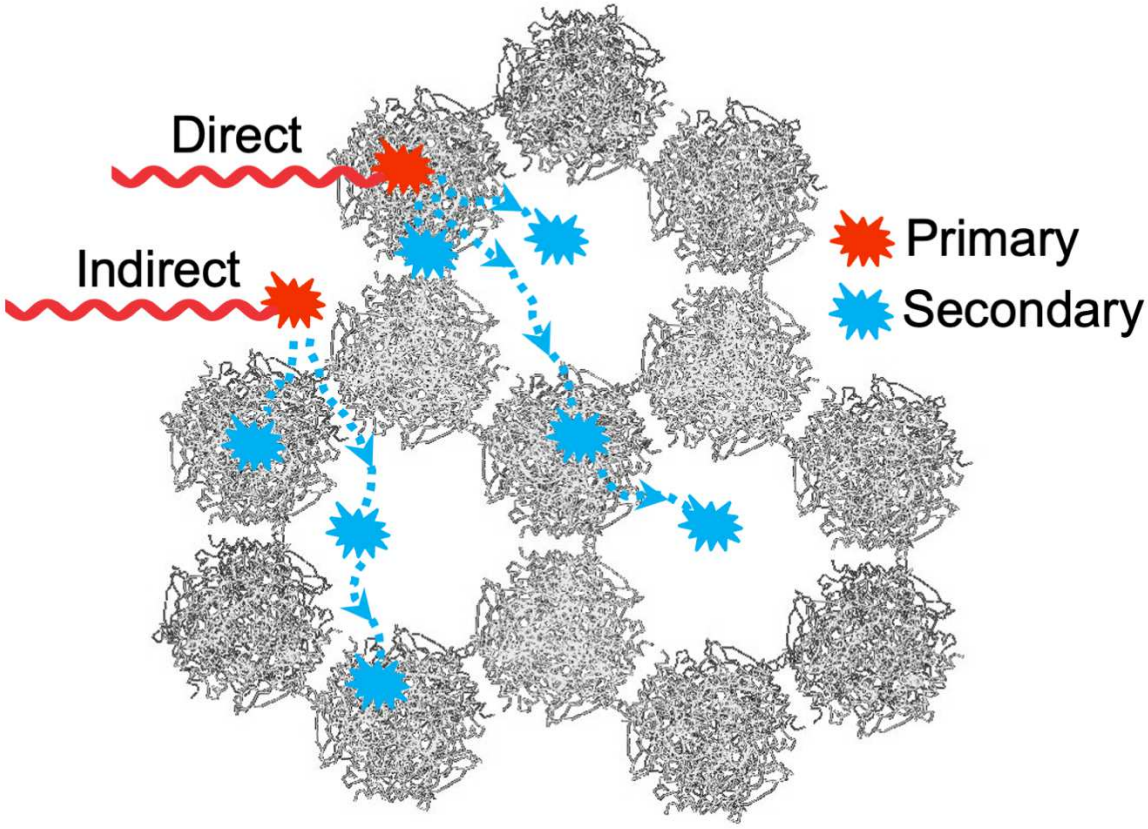

Figure 1: Diagrammatic representation of the interaction of X-rays with an acetylcholinesterase protein crystal (PDB code 1EA5) showing direct (on protein) / indirect (on solvent) and primary (red stars) / secondary (blue stars) events. Elastic (Thompson) scattering leaves no energy in the crystal and thus causes no damage.

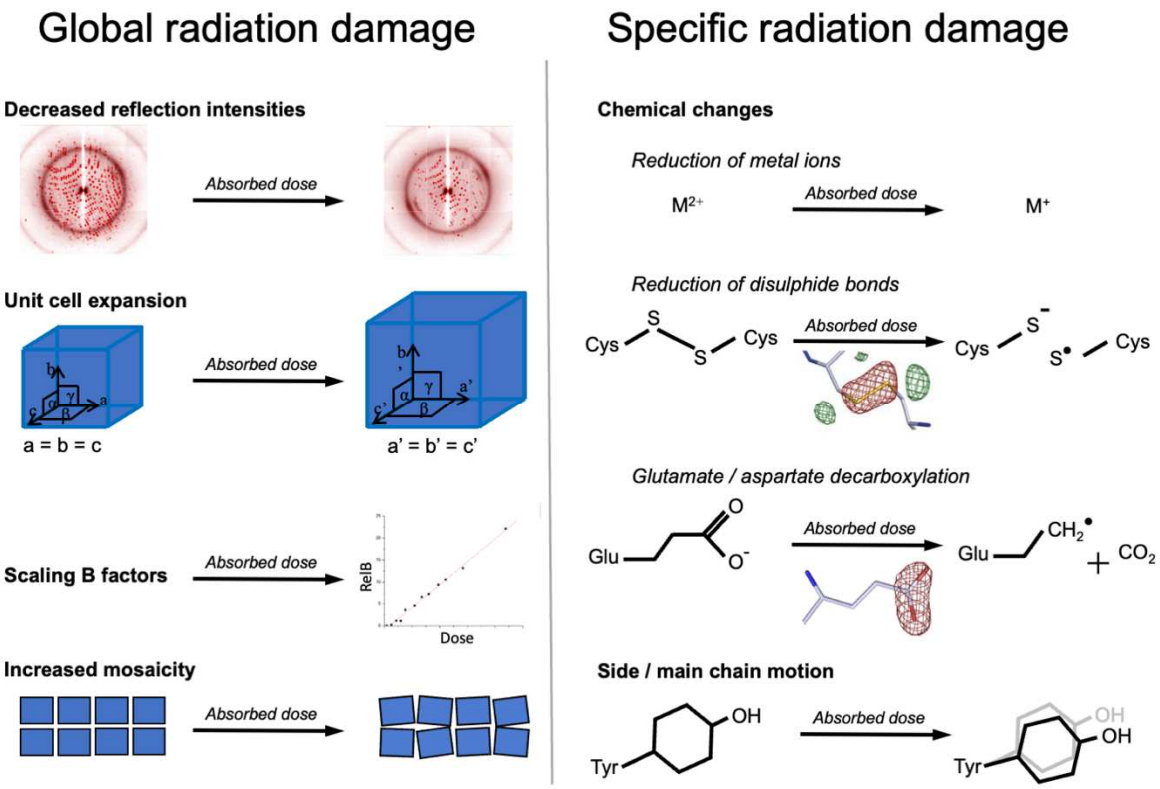

Figure 2: Illustrative summary of global and specific radiation damage pathologies observed at 100 K.

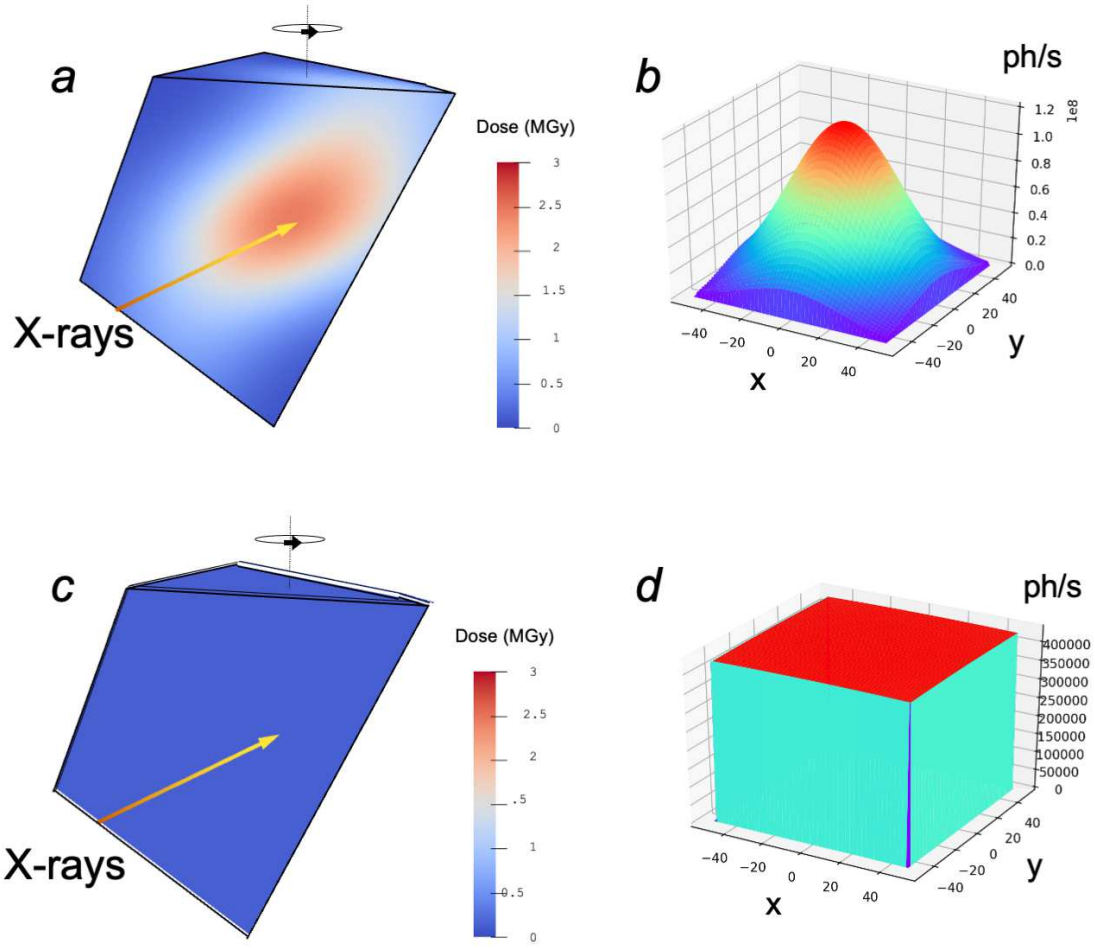

Figure 3: RADDOSE-3D calculated dose distributions for a protein crystal rotated 180° while irradiated in X-ray beams with two different profiles. (*a, b*) in a typical Gaussian profile resulting in inhomogeneous irradiation and dose values varying between 0 and 3 MGy, and (*c,d*) in a top-hat profile (e.g. from EMBL beamline P14, PETRA III, DESY, Hamburg) giving a homogeneous dose distribution of less than 0.5 MGy.

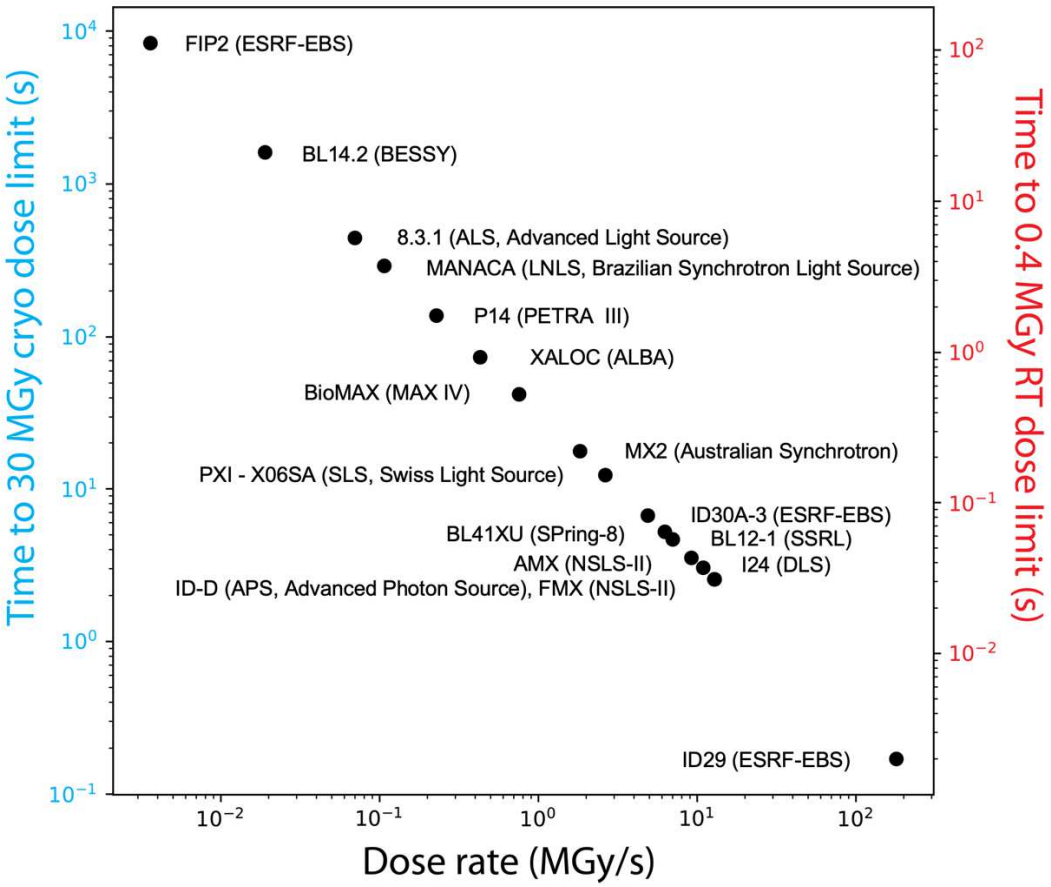

Figure 4: Plot of dose rate against time taken to reach the 100 K experimental dose limit of 30 MGy[17] (left axis) and the RT limit of 0.4 kGy•[33] (right axis) at various MX synchrotron beamlines. Average diffraction weighted doses (DWD) were calculated for a (50 µm)^3 lysozyme crystal (grown in 100 mM NaAc and 1M NaCl, solvent fraction 38%) rotated 360° in the flux within the FWHMs of the various beams. Necessary data, such as beam shape (Gaussian if not stated otherwise), beam size (FWHM, h (µm) × v (µm), flux in whole beam profile (photons/s) and photon energy (keV) at which flux was measured were provided in April 2023 by the beamline scientists at each facility: FIP2 (top hat, 200×200, 5×10^11, 12.6), BL14.2 (90×70, 4×10^11, 13.5), 8.3.1 (60×80, 8×10^11, 11.1), MANACA (20×20, 3×10^11, 12.7), P14 (top-hat, 100×100, 8×10^12, 12.7), XALOC (50×25, 2×10^12, 12.7), BioMAX (50×50, 7×10^12, 12.7), MX2 (22×10, 2×10^12, 13.0), PXI-X06SA (20×5, 2×10^12, 12.4), ID30A-3 (15×18, 1×10^13, 12.8), BL41XU (20×20, 2×10^13, 12.4), BL12-1 (40×5, 4×10^12, 10.9), AMX (7×5, 4×10^12, 13.5), I24 (8×8, 8×10^12, 12.4), ID-D (50×5, 1×10^13, 12.0), FMX (5×3, 4×10^12, 12.7), ID29 (4x2, 5x10^15, 11.6).

References

[1] Garman EF, Schneider TR. Macromolecular Cryocrystallography. Journal of Applied Crystallography 1997; 30:211-237.

[2] Taube M, Pietralik Z, Szymanska A *et al.* The domain swapping of human cystatin C induced by synchrotron radiation. Sci Rep 2019; 9:8548.

•[3] Stachowski T, Grant TD, Snell EH. Structural consequences of transforming growth factor beta-1 activation from near-therapeutic X-ray doses. J Synchrotron Radiat 2019; 26:967-979.

This low dose SAXS study reported the dimer-to-monomer dose dependent X-ray induced bond cleavage and fragmentation at near physiological conditions of a protein (transforming growth factor beta 1, TGFβ-1) engineered to dimerise through a susceptible disulphide bond. The results shed light on the structural dynamics of X-ray radiation induced TGFβ-1 activation and are relevant to understanding the cellular response to radiation.

••[4] Ebrahim A, Moreno-Chicano T, Appleby MV *et al.* Dose-resolved serial synchrotron and XFEL structures of radiation-sensitive metalloproteins. IUCrJ 2019; 6:543-551.

X-ray irradiation induced elongation of a Fe-water bond in a highly radiation sensitive metallo-protein is studied by SSX as a function of the absorbed dose and compared to the bond length determined by damage free SFX at an XFEL. This comparison is made possible by using similarly sized DtpAa microcrystals presented to the X-ray beams at RT with the same solid support system. Even at the lowest X-ray dose (33 kGy per data set) the SSX structure already shows an elongated Fe-water bond. Zero-dose extrapolation of the SSX bond lengths yields the value determined in the pristine metallo protein by SFX.

[5] Ebrahim A, Appleby MV, Axford D *et al.* Resolving polymorphs and radiation-driven effects in microcrystals using fixed-target serial synchrotron crystallography. Acta Crystallographica Section D 2019; 75:151-159.

[6] Pfanzagl V, Beale JH, Michlits H *et al.* X-ray-induced photoreduction of heme metal centers rapidly induces active-site perturbations in a protein-independent manner. J Biol Chem 2020; 295:13488-13501.

[7] Tandrup T, Muderspach SJ, Banerjee S *et al.* Changes in active-site geometry on X-ray photoreduction of a lytic polysaccharide monooxygenase active-site copper and saccharide binding. IUCrJ 2022; 9:666-681.

[8] Zárate-Romero A, Stojanoff V, Cohen AE *et al.* X-ray driven reduction of Cpd I of Catalase-3 from N. crassa reveals differential sensitivity of active sites and formation of ferrous state. Archives of Biochemistry and Biophysics 2019; 666:107-115.

[9] Burgie ES, Clinger JA, Miller MD *et al.* Photoreversible interconversion of a phytochrome photosensory module in the crystalline state. Proceedings of the National Academy of Sciences 2020; 117:300.

[10] Dubnovitsky AP, Ravelli RB, Popov AN, Papageorgiou AC. Strain relief at the active site of phosphoserine aminotransferase induced by radiation damage. Protein Sci 2005; 14:1498-1507. Epub 2005 May 1499.

[11] Schlichting I, Berendzen J, Chu K *et al.* The catalytic pathway of cytochrome p450cam at atomic resolution. Science 2000; 287:1615-1622.

[12] Berglund GI, Carlsson GH, Smith AT *et al.* The catalytic pathway of horseradish peroxidase at high resolution. Nature 2002; 417:463-468.

[13] Polyakov KM, Gavryushov S, Ivanova S *et al.* Structural study of the X-ray-induced enzymatic reduction of molecular oxygen to water by Steccherinum murashkinskyi laccase: insights into the reaction mechanism. Acta Crystallographica Section D 2017; 73:388-401.

[14] von Stetten D, Giraud T, Carpentier P *et al.* In crystallo optical spectroscopy (icOS) as a complementary tool on the macromolecular crystallography beamlines of the ESRF. Acta crystallographica. Section D, Biological crystallography 2015; 71:15-26.

[15] E. Cohen A, Doukov T, S. Soltis M. UV-Visible Absorption Spectroscopy Enhanced X-ray Crystallography at Synchrotron and X-ray Free Electron Laser Sources. Protein and Peptide Letters 2016; 23:283-290.
[16] Bury CS, Carmichael I, Garman EF. OH cleavage from tyrosine: debunking a myth. Journal of Synchrotron Radiation 2017; 24:7-18.
[17] Owen RL, Rudino-Pinera E, Garman EF. Experimental determination of the radiation dose limit for cryocooled protein crystals. Proc Natl Acad Sci U S A. 2006; 103:4912-4917. Epub 2006 Mar 4920.
•[18] Gotthard G, Aumonier S, De Sanctis D *et al.* Specific radiation damage is a lesser concern at room temperature. IUCrJ 2019; 6:665-680.
This systematic study combines X-ray crystallography and online Raman and UV-vis *in crystallo* microspectrophotometry to study the radiation sensitivity of three crystalline proteins at both 100 K and RT as a function of the absorbed dose. Global and specific X-ray radiation damage is shown to be largely decoupled at 100 K, with specific damage occurring one to three orders of magnitude lower in dose than global damage, compared with only a factor of below 10 at RT, indicating that specific and global damage occur on similar dose scales.

•[19] Bugris V, Harmat V, Ferenc G *et al.* Radiation-damage investigation of a DNA 16-mer. Journal of Synchrotron Radiation 2019; 26:998-1009.
A series of six 100 K structures derived from data collected from a 16-mer DNA crystal is analysed for both global and specific RD. It is concluded that, compared to the rate of damage to lysozyme crystals from which data were collected under identical conditions, the 16-mer DNA crystal was less sensitive to both global and specific RD In terms of the latter, the damaged sites were concentrated around the bound calcium atoms that had been sequestered from the crystallisation buffer.

[20] Warren AJ, Axford D, Owen RL. Direct measurement of X-ray-induced heating of microcrystals. Journal of Synchrotron Radiation 2019; 26:991-997.
[21] Owen RL, Axford D, Nettleship JE *et al.* Outrunning free radicals in room-temperature macromolecular crystallography. Acta Crystallographica Section D 2012; 68:810-818.
[22] Warkentin M, Thorne RE. Glass transition in thaumatin crystals revealed through temperature-dependent radiation-sensitivity measurements. Acta Crystallogr D Biol Crystallogr 2010; 66:1092-1100.
[23] Warkentin MA, Atakisi H, Hopkins JB *et al.* Lifetimes and spatio-temporal response of protein crystals in intense X-ray microbeams. IUCrJ 2017; 4:785-794.
•[24] Atakisi H, Conger L, Moreau DW, Thorne RE. Resolution and dose dependence of radiation damage in biomolecular systems. IUCrJ 2019; 6:1040-1053.
A model for diffracted intensity decay based on physical considerations is described and tested against three published 100 K datasets. Intensity decay was consistent with exponential decay in which the negative exponent is directly proportional to the dose and inversely proportional to the diffraction wavevector, q, raised to the power (α) of ~1.7. The physical interpretation proposed for this model is that local absorption of energy at random places causes electron density blurring in a small volume, and it results in a prediction that $\alpha \sim 2$. It is shown that appropriate models are highly dependent on the profile of the incident beam and that for a Gaussian-shape the dose becomes almost independent of the actual dose at large doses due to 'hole-burning' by the intense beam centre where damaged regions no longer diffract to high resolution.

[25] Holton JM. A beginner's guide to radiation damage. J Synchrotron Radiat. 2009; 16:133-142. Epub 2009 Feb 2025.
•[26] Bhattacharyya R, Dhar J, Ghosh Dastidar S *et al.* The susceptibility of disulfide bonds towards radiation damage may be explained by S...O interactions. IUCrJ 2020; 7:825-834.

The study examines the correlation between features in the local environments of disulphide bonds in crystalline proteins and the frequently reported differential radiation sensitivity of these disulphide bonds. The location of a carbonyl O atom along the extension of the disulphide bond is shown to increase its sensitivity to radiation-induced cleavage by providing an electron transfer pathway. The normally stabilising S ··· O interaction thus appears to decrease disulphide stability under X-ray irradiation.

[27] van den Bedem H, Wilson MA. Shining light on cysteine modification: connecting protein conformational dynamics to catalysis and regulation. Journal of Synchrotron Radiation 2019; 26:958-966.
[28] Blake CCF, Philips DC. Biological Effects of Ionizing Radiation at the Molecular Level. Vienna: International Atomic Energy Agency. 1962:183 - 191.
[29] Nave C, Garman EF. Towards an understanding of radiation damage in cryocooled macromolecular crystals. J Synchrotron Radiat 2005; 12:257-260. Epub 2005 Apr 2014.
[30] Helliwell JR. Protein crystal perfection and the nature of radiation damage. J. Cryst. Growth 1988; 90:259-272.
[31] Gati C, Bourenkov G, Klinge M *et al.* Serial crystallography on in vivo grown microcrystals using synchrotron radiation. IUCrJ 2014; 1:87-94.
[32] Botha S, Nass K, Barends TR *et al.* Room-temperature serial crystallography at synchrotron X-ray sources using slowly flowing free-standing high-viscosity microstreams. Acta Crystallogr D Biol Crystallogr 2015; 71:387-397.
•[33] de la Mora E, Coquelle N, Bury CS *et al.* Radiation damage and dose limits in serial synchrotron crystallography at cryo- and room temperatures. P Natl Acad Sci USA 2020; 117:4142-4151.
Between 40 and 90 full X-ray crystallographic data sets were collected on microcrystals of HEWL by serial synchrotron crystallography (SSX) at 100 K and at RT, with a total absorbed dose per data set as low as 5 kGy. Global damage and specific damage to disulphide bonds, evident in Fourier difference maps, is quantified as a function of absorbed dose. At RT, specific disulphide damage first increases and then apparently decreases as a function of dose, a peculiar behaviour explained by hole burning [42] of the sample by the central part of the X-ray beam. As a rough guide line, in order to minimise global and specific damage to disulphide bonds, experimenters are advised not to exceed doses of 0.4 and 0.08 MGy in static and time-resolved SSX experiments at RT, respectively.

[34] Fischer M. Macromolecular room temperature crystallography. Q Rev Biophys 2021; 54:e1.
[35] Southworth-Davies RJ, Medina MA, Carmichael I, Garman EF. Observation of decreased radiation damage at higher dose rates in room temperature protein crystallography. Structure. 2007; 15:1531-1541.
[36] Coquelle N, Brewster AS, Kapp U *et al.* Raster-scanning serial protein crystallography using micro- and nano-focused synchrotron beams. Acta Crystallographica Section D 2015; 71:1184-1196.
[37] Russi S, Gonzalez A, Kenner LR *et al.* Conformational variation of proteins at room temperature is not dominated by radiation damage. Journal of Synchrotron Radiation 2017; 24:73-82.
[38] Schubert R, Kapis S, Gicquel Y *et al.* A multicrystal diffraction data-collection approach for studying structural dynamics with millisecond temporal resolution. IUCrJ 2016; 3:393-401.
[39] Roedig P, Duman R, Sanchez-Weatherby J *et al.* Room-temperature macromolecular crystallography using a micro-patterned silicon chip with minimal background scattering. Journal of Applied Crystallography 2016; 49:968-975.
[40] Suzuki R, Baba S, Mizuno N *et al.* Radiation-induced defects in protein crystals observed by X-ray topography. Acta Crystallogr D Struct Biol 2022; 78:196-203.
[41] Teng T, Moffat K. Primary radiation damage of protein crystals by intense synchrotron radiation. J. Synchrotron Rad. 2000; 7:313-317.
[42] Fraser JS, van den Bedem H, Samelson AJ *et al.* Accessing protein conformational ensembles using room-temperature X-ray crystallography. Proc Natl Acad Sci U S A 2011; 108:16247-16252.

[43] Yabukarski F, Doukov T, Mokhtari DA *et al.* Evaluating the impact of X-ray damage on conformational heterogeneity in room-temperature (277 K) and cryo-cooled protein crystals. Acta Crystallogr D Struct Biol 2022; 78:945-963.
[44] Gerstel M, Deane CM, Garman EF. Identifying and quantifying radiation damage at the atomic level. Journal of Synchrotron Radiation 2015; 22:201-212.
••[45] Shelley KL, Garman EF. Quantifying and comparing radiation damage in the Protein Data Bank. Nat Commun 2022; 13:1314.
Here, a new metric, B_{net}, is introduced and validated on 23 different crystal structures previously characterized as damaged. By comparing the B-factor values of damage-prone (oxygens from glutamate and aspartate residues) and non-damage-prone atoms in a similar local environment, B_{net} summarises in a single value the extent of damage suffered by a crystal structure. A B_{net} analysis of 93,978 cryo-cooled crystal structures deposited in the PDB is presented.

[46] Svensson O, Malbet-Monaco S, Popov A *et al.* Fully automatic characterization and data collection from crystals of biological macromolecules. Acta Crystallogr D 2015; 71:1757-1767.
[47] Hirata K, Yamashita K, Ueno G *et al.* ZOO: an automatic data-collection system for high-throughput structure analysis in protein microcrystallography. Acta Crystallogr D 2019; 75:138-150.
[48] Bury CS, Brooks-Bartlett JC, Walsh SP, Garman EF. Estimate your dose: RADDOSE-3D. Protein Science 2018; 27:217-228.
[49] Dickerson JL, Garman EF. Doses for experiments with microbeams and microcrystals: Monte Carlo simulations in RADDOSE-3D. Protein Sci 2021; 30:8-19.
[50] Taberman H, Bury CS, van der Woerd MJ *et al.* Structural knowledge or X-ray damage? A case study on xylose isomerase illustrating both. Journal of Synchrotron Radiation 2019; 26:931-944.
[51] Flot D, Mairs T, Giraud T *et al.* The ID23-2 structural biology microfocus beamline at the ESRF. Journal of Synchrotron Radiation 2010; 17:107-118.
[52] Zander U, Bourenkov G, Popov AN *et al.* MeshAndCollect: an automated multi-crystal data-collection workflow for synchrotron macromolecular crystallography beamlines. Acta Crystallographica Section D 2015; 71:2328-2343.
[53] Halsted TP, Yamashita K, Gopalasingam CC *et al.* Catalytically important damage-free structures of a copper nitrite reductase obtained by femtosecond X-ray laser and room-temperature neutron crystallography. IUCrJ 2019; 6:761-772.
[54] Moreno-Chicano T, Carey LM, Axford D *et al.* Complementarity of neutron, XFEL and synchrotron crystallography for defining the structures of metalloenzymes at room temperature. IUCrJ 2022; 9.
[55] Barends TRM, Stauch B, Cherezov V, Schlichting I. Serial femtosecond crystallography. Nature Reviews Methods Primers 2022; 2:59.
[56] Nave C, Hill MA. Will reduced radiation damage occur with very small crystals? J Synchrotron Radiat 2005; 12:299-303. Epub 2005 Apr 2014.
[57] Dickerson JL, Garman EF. The potential benefits of using higher X-ray energies for macromolecular crystallography. Journal of Synchrotron Radiation 2019; 26:922-930.
[58] Storm SLS, Crawshaw AD, Devenish NE *et al.* Measuring energy-dependent photoelectron escape in microcrystals. IUCrJ 2020; 7:129-135.
••[59] Storm SLS, Axford D, Owen RL. Experimental evidence for the benefits of higher X-ray energies for macromolecular crystallography. IUCrJ 2021; 8:896-904.
Experimental evidence is presented validating the prediction that using higher incident X-ray energy should result in higher diffraction efficiency (DE: total number of elastically scattered photons/absorbed dose) if a suitable detector is employed. Measurements at 12.4 and 25 keV using an Eiger CdTe detector demonstrated that the DE increased by a factor of more than two at the higher Ex and that higher resolution data could be collected for the same dose. When the same experiment was repeated using a Si PILATUS detector, no gain in DE was recorded due to the lower DQE of that detector at higher energies.

[60] Ueno G, Shimada A, Yamashita E *et al.* Low-dose X-ray structure analysis of cytochrome c oxidase utilizing high-energy X-rays. Journal of Synchrotron Radiation 2019; 26:912-921.
[61] Zeldin OB, Brockhauser S, Bremridge J *et al.* Predicting the X-ray lifetime of protein crystals. Proc Natl Acad Sci U S A 2013; 110:20551-20556.
[62] Brooks-Bartlett JC. Quantifying radiation damage in X-ray diffraction experiments in structural biology. In: University of Oxford; 2016.
[63] Tosha T, Nomura T, Nishida T *et al.* Capturing an initial intermediate during the P450nor enzymatic reaction using time-resolved XFEL crystallography and caged-substrate. Nat Commun 2017; 8:1585.
[64] Sorigue D, Hadjidemetriou K, Blangy S *et al.* Mechanism and dynamics of fatty acid photodecarboxylase. Science 2021; 372.
[65] Maestre-Reyna M, Yang CH, Nango E *et al.* Serial crystallography captures dynamic control of sequential electron and proton transfer events in a flavoenzyme. Nat Chem 2022; 14:677-685.
[66] Srinivas V, Banerjee R, Lebrette H *et al.* High-Resolution XFEL Structure of the Soluble Methane Monooxygenase Hydroxylase Complex with its Regulatory Component at Ambient Temperature in Two Oxidation States. Journal of the American Chemical Society 2020; 142:14249-14266.
[67] Nass K. Radiation damage in protein crystallography at X-ray free-electron lasers. Acta Crystallographica Section D 2019; 75.
[68] Lomb L, Barends TR, Kassemeyer S *et al.* Radiation damage in protein serial femtosecond crystallography using an x-ray free-electron laser. Physical review. B, Condensed matter and materials physics 2011; 84:214111.
[69] Nass K, Foucar L, Barends TR *et al.* Indications of radiation damage in ferredoxin microcrystals using high-intensity X-FEL beams. J Synchrotron Radiat 2015; 22:225-238.
••[70] Nass K, Gorel A, Abdullah MM *et al.* Structural dynamics in proteins induced by and probed with X-ray free-electron laser pulses. Nat Commun 2020; 11:1814.
In this time-resolved X-ray pump/X-ray probe experiment on protein nanocrystals, two pulses with different photon energies which lay above and below the Fe K-edge were chosen, so that the pump, but not the probe pulses were absorbed by a thin Fe foil in front of the detector. With pump-probe delays increasing from 20 to 100 fs, global radiation damage, as well as specific structural changes such as lengthening of disulphide bonds is observed. Due to the femtosecond time scale, radiation chemistry considerations point to disulphide bond elongation being due to oxidative processes, rather than reductive ones as observed in MX. Theoretical analysis highlights the effects of ion caging and plasma ions on the structural dynamics of X-ray induced disulphide bond lengthening.

•[71] Dickerson JL, McCubbin PTN, Garman EF. RADDOSE-XFEL: femtosecond time-resolved dose estimates for macromolecular X-ray free-electron laser experiments. Journal of Applied Crystallography 2020; 53:549-560.
An extension of the dose estimating software tool, RADDOSE-3D, called RADDOSE-XFEL is described. It allows the calculation of time-resolved absorbed doses during XFEL experiments, and could be used to facilitate the study of radiation damage at XFELs so that experimenters could plan their experiments to avoid radiation damage manifesting in their structures.

[72] Paquete-Ferreira J, Leisico F, Correia MAS *et al.* Using Small-angle X-ray Scattering to Characterize Biological Systems: A General Overview and Practical Tips. Methods Mol Biol 2023; 2652:381-403.
[73] Christensen J, Horton PN, Bury CS *et al.* Radiation damage in small-molecule crystallography: fact not fiction. IUCrJ 2019; 6:703-713.

[74] Fernando NK, Cairns AB, Murray CA *et al.* Structural and Electronic Effects of X-ray Irradiation on Prototypical [M(COD)Cl]2 Catalysts. The Journal of Physical Chemistry A 2021; 125:7473-7488.
[75] Fernando NK, Boström HLB, Murray CA *et al.* Variability in X-ray induced effects in [Rh(COD)Cl](2) with changing experimental parameters. Phys Chem Chem Phys 2022; 24:28444-28456.
[76] Schriber EA, Paley DW, Bolotovsky R *et al.* Chemical crystallography by serial femtosecond X-ray diffraction. Nature 2022; 601:360-365.
[77] Baker LA, Rubinstein JL. Chapter Fifteen - Radiation Damage in Electron Cryomicroscopy. In: Methods in Enzymology. Edited by: Jensen GJ. Academic Press; 2010. pp. 371-388.
[78] Kühlbrandt W. The Resolution Revolution. Science 2014; 343:1443-1444.
[79] Bartesaghi A, Matthies D, Banerjee S *et al.* Structure of beta-galactosidase at 3.2-A resolution obtained by cryo-electron microscopy. Proc Natl Acad Sci U S A 2014; 111:11709-11714.
[80] Henderson R. The potential and limitations of neutrons, electrons and X-rays for atomic resolution microscopy of unstained biological molecules. Q Rev Biophys 1995; 28:171-193.
•[81] Kato K, Miyazaki N, Hamaguchi T *et al.* High-resolution cryo-EM structure of photosystem II reveals damage from high-dose electron beams. Communications Biology 2021; 4:382.
Photosystem II structures are determined by single particle cryo EM at different absorbed doses and compared to a radiation damage free photosystem II structure determined by SFX at an XFEL. Using the initial 1 - 24 movie frames, corresponding to a total of 83 $e^-/Å^2$ (307 MGy), a resolution of 1.95 Å is achieved. The Mn-O and Mn-Mn distances are 0.1 – 0.4 Å longer than in the corresponding SFX structure. When only the initial two movie frames are used, corresponding to a total of 3.3 $e^-/Å^2$ (12.2 MGy), the resolution only marginally drops (to 2.08 Å). The Mn-O and Mn-Mn distances are now close to those in the SFX structure, yet still somewhat longer, indicating that this low-dose single particle cryo EM structure is still not completely damage free.

[82] Peet MJ, Henderson R, Russo CJ. The energy dependence of contrast and damage in electron cryomicroscopy of biological molecules. Ultramicroscopy 2019; 203:125-131.
[83] Naydenova K, Kamegawa A, Peet MJ *et al.* On the reduction in the effects of radiation damage to two-dimensional crystals of organic and biological molecules at liquid-helium temperature. Ultramicroscopy 2022; 237:113512.
[84] Zhang Y, Lu PH, Rotunno E *et al.* Single-particle cryo-EM: alternative schemes to improve dose efficiency. J Synchrotron Radiat 2021; 28:1343-1356.
[85] Naydenova K, Jia P, Russo CJ. Cryo-EM with sub–1 Å specimen movement. Science 2020; 370:223-226.
[86] Clabbers MTB, Shiriaeva A, Gonen T. MicroED: conception, practice and future opportunities. IUCrJ 2022; 9:169-179.
••[87] Hattne J, Shi D, Glynn C *et al.* Analysis of Global and Site-Specific Radiation Damage in Cryo-EM. Structure 2018; 26:759-766.e754.
This a systematic study of global and site-specific electron radiation damage at 100 K to a nanocrystalline protein (proteinase K) and a short hepta-peptide with a bound metal in MicroED experiments. By minimising the exposure fluence, data could be collected repeatedly over the same wedge of reciprocal space so that damage progression can be visualised. Specific damage to the metal, disulphide bonds and acidic residues is observed, even at exposures below 1 e^- / $Å^2$ (equivalent to 4.5 MGy according to [77]).

[88] Martynowycz MW, Hattne J, Gonen T. Experimental Phasing of MicroED Data Using Radiation Damage. Structure 2020; 28:458-464.e452.
[89] Foos N, Seuring C, Schubert R *et al.* X-ray and UV radiation-damage-induced phasing using synchrotron serial crystallography. Acta Crystallographica Section D 2018; 74:366-378.

[90] Bücker R, Hogan-Lamarre P, Mehrabi P *et al.* Serial protein crystallography in an electron microscope. Nature Communications 2020; 11:996.
[91] Egerton RF. Dose measurement in the TEM and STEM. Ultramicroscopy 2021; 229:113363.